Received 17 September 2015; revised 6 November 2015 and 14 November 2015; accepted 22 November 2015. Date of publication 25 November 2015; date of current version 18 December 2015. The review of this paper was arranged by Editor M. Chan.

Digital Object Identifier 10.1109/JEDS.2015.2503922

Threshold Switching Characteristics of $Nb/NbO_2/TiN$ Vertical Devices

YUHAN WANG[1], RYAN B. COMES[2], STUART A. WOLF[1,3] (Member, IEEE), AND JIWEI LU[1] (Member, IEEE)

1 Department of Materials Science and Engineering, University of Virginia, Charlottesville, VA 22904, USA
2 Fundamental and Computational Sciences Directorate, Pacific Northwest Laboratory, Richland, WA 99352, USA
3 Department of Physics, University of Virginia, Charlottesville, VA 22904, USA

CORRESPONDING AUTHOR: Y. WANG (e-mail: yw9ep@virginia.edu)

ABSTRACT We have observed threshold switching (TS) with minimal hysteresis and a small threshold electric field (60–90 kV/cm) in $Nb/NbO_2/TiN$ structures. The TS was unipolar with certain repeatability. A less sharp but still sizable change in the device resistance can be observed up to 150 °C. The TS without Nb capping layer exhibited hysteretic characteristics. It was proposed that the surface Nb_2O_5 layer on NbO_2 could significantly modify the TS in this vertical device. This understanding of the surface effect will allow further control of the non-linear IV characteristics for NbO_2-based switches or selector devices.

INDEX TERMS Niobium dioxide, threshold switching, metal-insulator transition.

I. INTRODUCTION

Threshold switching (TS) has been reported in niobium oxides since as early as the 1960s [1], including both NbO_2 [2] and metal-rich nonstoichiometric phases (NbO_x) [3]–[5]. Besides the TS triggered by electric field, NbO_2 also undergoes a metal-insulator transition (MIT) at ∼1081 K, which is accompanied by a first order phase transition from a distorted rutile structure (space group $I4_1/a$) to a rutile structure (space group $P4_2/mnm$) [6]. The TS and thermally induced MIT are similar to those of VO_2 (thermally induced MIT happens at ∼ 340 K) [7], with the higher transition temperature of NbO_2 promising more extended temperature range in circuit applications. The mechanism for the TS in NbO_2 remains controversial. Some suggested the TS was essentially the thermally driven MIT, which was induced by Joule heating and a conducting filament was formed [8]–[10], while others speculated that the TS was triggered by changes in electronic structures [2], [11].

Selector devices with a strong non-linearity in the IV characteristics can be critical components for vast "crosspoint" arrays, offering an avenue to dense nonvolatile memory devices [12]. The TS and MIT of NbO_2 makes it a promising candidate for the selector devices [13]–[16]. However, it has been a challenge to prevent the formation of Nb_2O_5 both in synthesis and after-growth fabrication of NbO_2, and the threshold voltages were still too large [12]. In this work, the novel reactive bias target ion beam deposition (RBTIBD) technique was used to synthesize phase pure NbO_2 films. The NbO_2 film was capped with a ∼100 nm thick Nb film *in-situ* to prevent the formation of an Nb_2O_5 overlayer observed previously on epitaxial NbO_2 films [17].

II. EXPERIMENT

NbO_2 films were deposited on TiN/Si(001) substrates by RBTIBD. The base pressure of the main chamber was $\sim 9\times10^{-8}$ Torr. The pressure during deposition was $\sim 1\times10^{-3}$ Torr and the substrates were heated to 500 °C. An Ar/O_2 80/20 mixture was used as the reactive gas. NbO_2 films in this work were grown with the flow of the reactive mixture being set to 5.5 SCCM. Detailed procedures of deposition can be found elsewhere [17]. The thickness of the grown films was obtained by X-ray reflectivity (Smart Lab, Rigaku Inc.) and the growth rate of the NbO_2 film was ∼3.5 nm/min. In some samples, a ∼100 nm thick Nb layer was deposited at room temperature on top of NbO_2 prior to air exposure.

The microstructure of the NbO_2 film was examined by a 2θ X-Ray diffraction scan with a Cu $K\alpha_1$ radiation, and the Raman spectrum was measured by an inVia Raman microscope with a 514 nm laser source. The XPS spectra

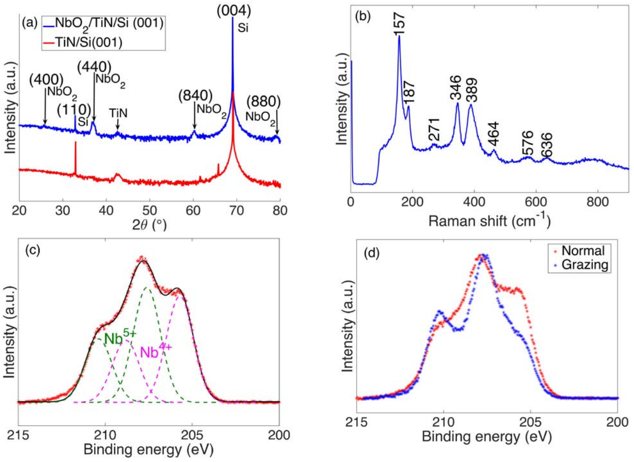

FIGURE 1. **(a) XRD 2θ scans of NbO$_2$ film (top) and TiN/Si(001) substrate (bottom). (b) Raman spectrum of NbO$_2$ film deposited on TiN/Si(001) substrate. (c) Core level Nb 3d spectrum of NbO$_2$ film with normal photoelectron incidence. (d) Normalized Core level Nb 3d spectra of NbO$_2$ film obtained at photoelectron incident angle 90° (Normal) Vs 20° (Grazing).**

were measured with monochromatic Al Kα radiation at base pressure of 1×10^{-9} Torr.

Switching of the Nb/NbO$_2$/TiN stacks was performed on a two-terminal structure. The capping layer served as a top contact with different sizes defined by the photolithographic technique and reactive ion etching. The bottom electrode was the TiN layer to which the contact was made by cold-pressing indium via scratches into the substrate at the corners of the samples. Pulsed sweeps of voltage were conducted using a Keithley 2635 source meter with tungsten tip (diameter = 5 μm), with pulse-on time of 1 ms and pulse-off time of 10 ms.

III. RESULTS AND DISCUSSION

Fig. 1(a) shows the XRD 2θ scan of the deposited NbO$_2$ film without Nb cap. Only diffraction peaks from tetragonal NbO$_2$ were observed [18]. The Raman spectrum of the NbO$_2$ film shown in Fig. 1(b) matched well to the previous reported spectra of NbO$_2$ films [17], [19], which suggested predominant existence of NbO$_2$. Fig. 1(c) shows the core level 3d spectrum measured with the photoelectron emission normal to the film surface. The primary peaks corresponded to Nb^{5+} and Nb^{4+} peaks, respectively. No Nb^{2+} peaks were observed. To determine whether Nb^{5+} was limited to the surface due to atmospheric exposure, the sample was tilted to make the photoelectron emission come from a grazing angle at 20°. As is shown in Fig. 1(d), the Nb^{4+} peaks are considerably depressed in the spectrum measured at incident angle of 20°, indicating that the film surface was over-oxidized to Nb^{5+} and Nb^{4+} should have significantly higher intensity in the bulk of the film. By applying similar analysis as in previous study [17], the surface Nb$_2$O$_5$ layer was estimated to be ~2 nm.

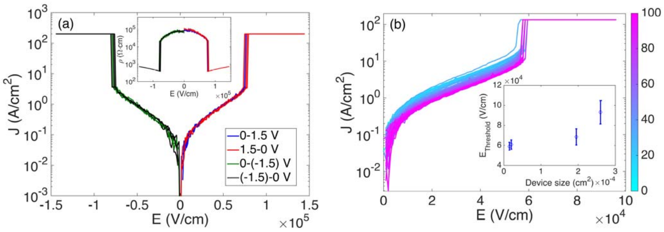

FIGURE 2. **(a) Typical current density-electric field (J-E) characteristics of Nb/NbO$_2$/TiN devices. The inset shows corresponding resistivity-electric field (ρ-E) characteristics; (b) Current density-electric field (J-E) characteristics of of 100 times voltage driven switches of Nb/NbO$_2$/TiN devices. The inset shows variation of E$_{\text{Threshold}}$ with the sizes of Nb top contacts.**

Fig. 2(a) shows typical switching characteristics of the Nb/NbO$_2$/TiN device with the top contact size of 30 μm × 50 μm in the pulsed voltage driven switches at room temperature. Upon the upward voltage sweep, the current through the device showed a sudden jump from ~0.055 mA to the preset compliance current (3 mA) at the applied voltage of ~0.8 V, corresponding to the change in resistance from 1.4×10^4 Ω to 270 Ω. The electric field was calculated based on the NbO$_2$ film thickness (~104 nm). The current density and resistivity were calculated based on the dimensions of the fabricated Nb top electrodes, assuming uniform electric current distribution. The threshold electric field ($E_{Threshold}$) corresponding to the switching voltage was 7.7×10^4 V/cm. The current density (J) was ~0.03 A/cm^2 at the beginning of scan, increased to ~3.7 A/cm^2 at the onset of switching, and reached the compliance value after switching. The low resistance state relapsed to the initial high resistance state once the electric field was reduced below $E_{Threshold}$. Symmetric switching behaviors under opposite polarity of bias were observed, which is in good agreement with the reported unipolar TS in NbO$_2$ devices [16], [20]. However, it is worth noting that the hysteresis of the TS shown here was much smaller as compared to what has been reported previously [16].

To further characterize the consistency of the switches, multiple successive ramps of voltage were applied on the Nb/NbO$_2$/TiN devices. 100 cycles of voltage driven switches through a 30 μm × 50 μm device are plotted in Fig. 2(b). While effective switches are still maintained, it was shown that over the 100 switches $E_{Threshold}$ increased and the transition became more abrupt. To understand the reason for these changes, it would be useful to investigate the oxidation/reduction of the Nb/NbO$_2$ interface due to the migration of point defects under electric field [21]. Multiple voltage driven switches were also conducted through Nb/NbO$_2$/TiN devices with different sizes of Nb contacts. Dimensions of the top contacts investigated included 30 μm × 50 μm, 40 μm × 50 μm, 130 μm × 150 μm, 130 μm × 200 μm. As is shown in the inset of Fig. 2(b), the $E_{Threshold}$ increased with the area of the top electrode, from ~ 60 kV/cm for the 30 μm × 50 μm contact to ~ 90 kV/cm for the 130 μm × 200 μm contact. The mechanism for the area dependence of $E_{Threshold}$ is not entirely clear, but may be related to the non-uniform switching near the edges of

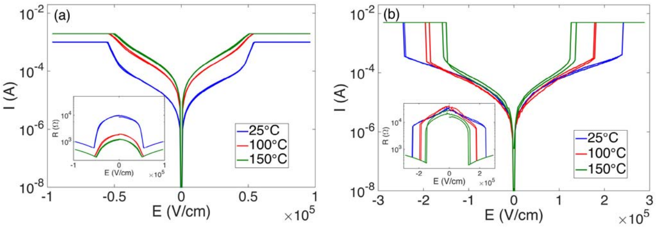

FIGURE 3. **(a) Current-electric field (I-E) characteristics of voltage driven switches in (a) Nb/NbO$_2$/TiN and (b) tip/NbO$_2$/TiN devices at different temperatures. The insets show corresponding resistance-electric field (Ω-E) characteristics.**

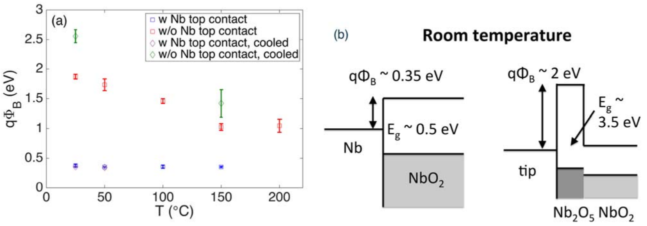

FIGURE 4. **(a) The barrier height ($q\Phi_B$) vs. temperature (T) characteristics and (b) proposed room temperature band diagrams for Nb/NbO$_2$/TiN and tip/NbO$_2$/TiN devices.**

the rectangular contact, since the distribution of electric field varies near electrodes.

Thermal stability of the TS was also investigated. As is shown in Fig. 3(a), TS of the devices could be obtained up to 150 °C, indicating the usefulness of such devices in circuit applications. With the increase of temperature, the switches became less sharp and the device resistance decreased, which is similar to earlier reports [10], [16]. Moreover, switching behaviors were also observed by using the probe tip to contact NbO$_2$ films directly at different temperatures (Fig. 3(b)). Forming processes occurred during the first sweep, in which the swept voltage ranges and threshold voltage values were larger than those in the following switches. While demonstrating TS and symmetric characteristics, the switching performed without Nb top contacts exhibited sharper switches with much larger $E_{Threshold}$ at each temperature. $E_{Threshold}$ with no Nb electrode at room temperature was ~250 kV/cm, which was close to the previously reported value [9]. It is also worth noting that the hysteresis loops were more visible in the switches conducted on the NbO$_2$ without Nb top contacts. Since sweeps on these two devices were performed under the same conditions, it is thus speculated that the difference was not due to Joule heating but related to the thin Nb$_2$O$_5$ layer on the exposed NbO$_2$.

To understand the difference between the TS behaviors of these two structures, the IV curves of high resistance state were fitted to different conduction models. It turned out the transport behavior under lower voltages can be well fitted by Simmons' equation [22], which describes the direct tunneling when two metallic electrodes are separated by a sufficiently thin insulating film. According to this model, the current density under intermediate voltage (V < Φ_B) is given by

$$\begin{aligned} J \sim (q\Phi_B - qV/2) \exp\left[-\frac{2d(2m)^{1/2}}{\hbar}(q\Phi_B - qV/2)^{1/2}\right] \\ - (q\Phi_B + qV/2) \exp\left[-\frac{2d(2m)^{1/2}}{\hbar}(q\Phi_B + qV/2)^{1/2}\right]. \end{aligned} \quad (1)$$

where $q\Phi_B$ is the barrier height, d is the insulator thickness, m is the effective mass, $\hbar$ is the reduced Plank constant. The extracted barrier height ($q\Phi_B$) as a function of temperature is plotted in Fig. 4(a). For Nb/NbO$_2$/TiN structure, $q\Phi_B$ was ~0.35 eV, and remained constant from room temperature to 150 °C. For the tip/NbO$_2$/TiN structure, $q\Phi_B$ was ~2 eV between room temperature and 100 °C, and was reduced to ~1 eV above 150 °C. It is clear that the contact/NbO$_2$ interface results in the very large difference in the values of $q\Phi_B$ obtained from the same sample. Schematics of the electronic structures for the devices with and without Nb capping layer at room temperature are proposed in Fig. 4(b). It appears that the *in-situ* Nb capping produced a clean contact interface between Nb/NbO$_2$, with minimal effect of Nb$_2$O$_5$. The energy barrier at this interface was ~0.35 eV which implies that the Fermi level of Nb is approximately in the middle of the band gap of NbO$_2$. When placing the tip on the area without Nb capping layer, the contact was made directly on the surface Nb$_2$O$_5$ rather than NbO$_2$. Nb$_2$O$_5$ is a well-known insulator with a band gap of ~3.3 eV [22], which is much larger than that of semiconducting NbO$_2$ (~0.5 eV). Due to the presence of the insulating Nb$_2$O$_5$, the barrier height was increased to ~2 eV. This also explains the larger $E_{Threshold}$ and hysteresis due to the more insulating nature of this thin Nb$_2$O$_5$ layer. The decrease of $q\Phi_B$ with temperature is related to the substantial diffusion of oxygen via the interstitial sites through Nb$_2$O$_5$, which has been observed in the oxides on the surface of single crystal Nb [23]. This understanding of modification effect from surface Nb$_2$O$_5$ promises better control on the TS characteristics of this vertical device, which can be integrated as a selecting device at every crosspoint in RRAM to solve the "sneak path" problem [12].

IV. CONCLUSION

In summary, we synthesized and fabricated Nb/NbO$_2$/TiN vertical devices with phase pure NbO$_2$ films. The TS obtained from the devices exhibited minimal hysteresis and symmetric behaviors under opposite polarity of bias. Moderate $E_{Threshold}$ was obtained (60 kV/cm-90 kV/cm), which showed a small dependence on the contact area. Reliable switches were retained over hundreds of times. Moreover, symmetric TS behaviors were also observed by using the probe tip to contact NbO$_2$ films directly, with much larger $E_{Threshold}$ (~ 250 kV/cm) and hysteresis. The TS characteristics were investigated as a function of temperature on both structures up to 150 °C. The Nb$_2$O$_5$ spontaneously formed on the exposed NbO$_2$ film was responsible for the difference between switches in these two structures. The fittings to the Simmons' model showed a significant difference for the barrier height for the vertical devices with and without the top Nb contact layer, which could be attributed to the surface Nb$_2$O$_5$ layer.

REFERENCES

[1] D. V. Geppert, "A new negative-resistance device," *Proc. IEEE*, vol. 51, no. 1, p. 223, Jan. 1963.

[2] G. C. Vezzoli, S. Levy, B. Lalevic, and M. Shoga, "Threshold switching polycrystalline NbO$_2$: Decay and recovery of the on state at room and low temperatures and its relationship to trapping centers," *J. Appl. Phys.*, vol. 54, no. 10, pp. 5828–5838, Oct. 1983.

[3] J. Bae *et al.*, "Coexistence of bi-stable memory and mono-stable threshold resistance switching phenomena in amorphous NbOx films," *Appl. Phys. Lett.*, vol. 100, no. 6, Feb. 2012, Art. ID 062902.

[4] X. Liu *et al.*, "Co-occurrence of threshold switching and memory switching in Pt/NbOx/Pt cells for crosspoint memory applications," *IEEE Electron Device Lett.*, vol. 33, no. 2, pp. 236–238, Feb. 2012.

[5] X. Liu *et al.*, "Complementary resistive switching in niobium oxide-based resistive memory devices," *IEEE Electron Device Lett.*, vol. 34, no. 2, pp. 235–237, Feb. 2013.

[6] R. F. Janninck and D. H. Whitmore, "Electrical conductivity and thermoelectric power of niobium dioxide," *J. Phys. Chem. Solids*, vol. 27, nos. 6–7, pp. 1183–1187, Jul. 1966.

[7] F. J. Morin, "Oxides which show a metal-to-insulator transition at the Neel temperature," *Phys. Rev. Lett.*, vol. 3, no. 1, pp. 34–36, Jul. 1959.

[8] M. D. Pickett and R. S. Williams, "Sub-100 fJ and sub-nanosecond thermally driven threshold switching in niobium oxide crosspoint nanodevices," *Nanotechnology*, vol. 23, no. 21, May 2012, Art. ID 215202.

[9] H. R. Philipp and L. M. Levinson, "NbO$_2$ devices for subnanosecond transient protection," *J. Appl. Phys.*, vol. 50, no. 7, pp. 4814–4822, Jul. 1979.

[10] S. Li, X. Liu, S. K. Nandi, D. K. Venkatachalam, and R. G. Elliman, "Temperature dependence of threshold switching in NbOx thin films," in *Proc. Optoelectron. Microelectron. Mater. Devices*, Perth, WA, Australia, 2014, pp. 138–140.

[11] S. H. Shin, T. Halpern, and P. M. Raccah, "High-speed high-current field switching of NbO$_2$," *J. Appl. Phys.*, vol. 48, no. 7, pp. 3150–3153, Jul. 1977.

[12] G. W. Burr *et al.*, "Access devices for 3D crosspoint memory," *J. Vac. Sci. Technol. B*, vol. 32, no. 4, Jul. 2014, Art. ID 040802.

[13] X. Liu *et al.*, "Diode-less bilayer oxide (WO(x)-NbO(x)) device for cross-point resistive memory applications," *Nanotechnology*, vol. 22, no. 47, 2011, Art. ID 475702.

[14] X. J. Liu *et al.*, "Reduced threshold current in NbO2 selector by engineering device structure," *IEEE Electron Device Lett.*, vol. 35, no. 10, pp. 1055–1057, Oct. 2014.

[15] S. K. Nandi, X. Liu, D. K. Venkatachalam, and R. G. Elliman, "Threshold current reduction for the metal–insulator transition in NbO$_{2-x}$-selector devices: The effect of ReRAM integration," *J. Phys. D Appl. Phys.*, vol. 48, no. 19, 2015, Art. ID 195105.

[16] S. Kim *et al.*, "Threshold-switching characteristics of a nanothin-NbO2-layer-based Pt/NbO2/Pt stack for use in cross-point-type resistive memories," *Microelectron. Eng.*, vol. 107, pp. 33–36, Jul. 2013.

[17] Y. Wang, R. B. Comes, S. Kittiwatanakul, S. A. Wolf, and J. Lu, "Epitaxial niobium dioxide thin films by reactive-biased target ion beam deposition," *J. Vac. Sci. Technol. A*, vol. 33, no. 2, Jan. 2015, Art. ID 021516.

[18] A. A. Bolzan, C. Fong, B. J. Kennedy, and C. J. Howard, "A powder neutron-diffraction study of semiconducting and metallic niobium dioxide," *J. Solid State Chem.*, vol. 113, no. 1, pp. 9–14, Nov. 1994.

[19] F. J. Wong, N. Hong, and S. Ramanathan, "Orbital splitting and optical conductivity of the insulating state of NbO$_2$," *Phys. Rev. B*, vol. 90, no. 11, Sep. 2014, Art. ID 115135.

[20] E. Cha *et al.*, "Nanoscale ($\sim$10nm) 3D vertical ReRAM and NbO2 threshold selector with TiN electrode," presented at the IEEE Int. Electron Devices Meeting (IEDM), Washington, DC, USA, 2013.

[21] S. M. Sadaf *et al.*, "Highly uniform and reliable resistance switching properties in bilayer WOx/NbOx RRAM devices," *Phys. Status Solidi A*, vol. 209, no. 6, pp. 1179–1183, 2012.

[22] Z. Weibin *et al.*, "The investigation of NbO2 and Nb2O5 electronic structure by XPS, UPS and first principles methods," *Surf. Interf. Anal.*, vol. 45, no. 8, pp. 1206–1210, Feb. 2013.

[23] M. Delheusy *et al.*, "X-ray investigation of subsurface interstitial oxygen at Nb/oxide interfaces," *Appl. Phys. Lett.*, vol. 92, no. 10, Mar. 2008, Art. ID 101911.

YUHAN WANG received the B.S. degree from Shandong University, Jinan, China, in 2010, and the M.S. degree from the University of Rochester, Rochester, NY, USA, in 2012. She is currently pursuing the Ph.D. degree with the Department of Materials Sciences and Engineering, University of Virginia, VA, USA. Her research activities focused on the metal insulator transition of niobium dioxide thin films.

RYAN B. COMES received the Ph.D. degree in engineering physics from the University of Virginia in 2013 and the B.S. degrees in physics and electrical and computer engineering from Carnegie Mellon University in 2008. He is a Linus Pauling Distinguished Post-Doctoral Fellow with the Physical and Computational Sciences Division, Pacific Northwest National Laboratory. His graduate research focused on the directed self-assembly of oxide nanocomposite thin films and was supported by a National Defense Science and Engineering Graduate Fellowship. His research focuses on the growth of oxide thin films by molecular beam epitaxy and characterization using X-ray photoelectron spectroscopy.

STUART A. WOLF received the A.B. degree from Columbia College in 1964, and the M.S. and PhD degrees from Rugters University in 1966 and 1969, respectively.

He was a Research Associate with Case Western Reserve University from 1970 to 1973 and a Visiting Scholar with UCLA. He was a Program Manager with DARPA and a Senior Scientist with the Naval Research Laboratory. He is the Director of the University of Virginia Institute for Nanoscale and Quantum Scientific and Technological Advanced Research and a Tenured Professor with the Materials Science and Engineering Department as well as the Physics Department. He has authored or co-authored two books, over 300 articles and has edited numerous conference proceedings. His research is in utilizing of the spin degree of freedom in novel oxide heterostructures that will utilize spin torque and electric fields to manipulate the magnetism in nanomagnetic heterostructures for both memory and logic.

He was a recipient of the NRL Sigma Xi Pure Science Award, the Navy Meritorious Civilian Service Award, and the E.H. Hulbert Award. He was a Divisional Councilor for the Condensed Matter Division from 1990 to 1991 and the Forum on Industrial and Applied Physics from 1993 to 1996. He was a Regent's Lecturer with the University of California and the Kilby Lecturer for the GOMAC Conference. He is a fellow of the APS in 1984.

JIWEI LU received the B.E. and M.E. degrees in materials science and engineering from Tsinghua University, Beijing, China, in 1999 and 2001, respectively, and the Ph.D. degree in materials science from the University of California, Santa Barbara, in 2006.

He is currently a Research Associate Professor with the Department of Materials Science and Engineering, University of Virginia, Charlottesville. His graduate research was centered on structure-property relationships of electric field tunable dielectric thin films, including strontium titanate and bismuth zinc niobate pyrochlores for microwave applications. His research is in the development of novel materials and structures which can be utilized as nonvolatile memory, reconfigurable logic, and very sensitive magnetic sensors.

Dr. Lu is a member of the American Physics Society and the Materials Research Society.